Transient Energy of an Individual Machine PART III: Newtonian Energy Conversion

SONGYAN WANG[ID]1, **JILAI YU**[ID]1, **AND AOIFE M. FOLEY**[ID]2, (Senior Member, IEEE)

[1]Department of Electrical Engineering, Harbin Institute of Technology, Harbin, Heilongjiang 150001, China
[2]School of Mechanical and Aerospace Engineering, Queen's University Belfast, Belfast BT7 1NN, U.K.

Corresponding author: Songyan Wang (wangsongyan@163.com)

ABSTRACT In this third paper, the fundamental mechanism of individual-machine transient stability is explained through Newtonian mechanics. The original Newtonian system with variant gravity is developed. This system is formed by a ball and the Earth. It is found that the Newtonian energy conversion strictly holds inside the system, and the equal area criterion can be considered a reflection of the Newtonian work. Based on these features, the stability characterizations of the system are given. Then, the original Newtonian system is extended to a generalized Newtonian system with multiple balls. It is found that this generalized Newtonian system can be decomposed into each two-ball-based subsystem, and the Newtonian energy conversion inside each subsystem is unique and different. This decomposition also ensures the independent parallel stability characterization of the generalized system. Finally, the strict mappings between Newtonian system stability and individual-machine transient stability are systematically analyzed. All these strict mappings fully reveal that the theoretical foundation of the individual-machine transient stability should be Newtonian mechanics.

INDEX TERMS Transient stability, transient energy, equal area criterion, individual machine.

NOMENCLATURE

KE	Kinetic energy
PE	Potential energy
RM	Reference machine
COI	Center of inertia
DLP	Dynamic liberation point
DSP	Dynamic stationary point
EAC	Equal area criterion
MPP	Maximum potential energy point
NEC	Newtonian energy conversion
SEP	Stable equilibrium point
TSA	Transient stability assessment
UEP	Unstable equilibrium point
IMKE	Individual-machine kinetic energy
IMPE	Individual-machine potential energy
IMTE	Individual-machine transient energy
IMTR	Individual-machine trajectory
IVCS	Individual-machine-virtual-COI-SYS machine system
RUEP	Relevant UEP
IMEAC	Individual-machine EAC
IMPES	Individual-machine potential energy surface

I. INTRODUCTION

A. LITERATURE REVIEW

Newtonian mechanics is crucial in classic physics. Conventionally, energy conversion is explained through the Newtonian system that is formed by a ball rolling inside a basin. The movement of the ball is depicted by using the equation of motion, and the conversion between kinetic energy (KE) and potential energy (PE) can be found through the motion of the ball. The ball will escape from the basin once it possesses residual KE at the edge of the basin. Essentially, the fierce motion of the ball is visually depicted through this Newtonian energy conversion (NEC).

In early transient stability studies, Athay discovered that transient behaviors of a power system cannot be explained effectively through Lyapunov theory [1]. Interestingly, Athay found that transient stability showed very strong similarities with Newtonian mechanics. That is, the mechanism of the trajectory stability of a multimachine system can be described through the conversion between "transient kinetic energy" and "transient potential energy". In this way, the transient stability is expressed as an energy ball rolling in an "energy basin", i.e., a potential energy surface [1]. Based on this visible Newtonian-mechanical description, the instability of the system is depicted as the ball escaping from the stability boundary, i.e., the potential energy boundary.

Furthermore, the Newtonian-like energy-type function, i.e., the transient energy function, is developed in the transient stability assessment (TSA). Following the thinking behind the transient energy function, the relevant-unstable-equilibrium-point (RUEP) method and the sustained fault method were developed [1]–[3]. However, the defect of the early transient energy function is that it is defined in a ''superimposed'' global manner. Under this superimposed definition, the NEC always fails because residual KE exists at the maximum potential energy point [4], [5]. To solve this problem, the KE correction technique [6], [7] and equivalent machine-based equal-area-criterion (EAC) methods [8], [9] were developed. Following this machine equivalence, the stability of the system is characterized precisely by using the EAC, and in this way, the residual KE problem is completely addressed. In brief, the thinking behind NEC unleashes transient stability studies from the restrictions of Lyapunov theory.

Motivated by the NEC in global methods, transient energy conversion can also be found inside each machine in a multimachine system [10], [11]. The partial energy function was developed, and the EAC of an individual machine was studied [12], [13]. It was conjectured that a distinctive individual-machine potential energy boundary might exist in the system [14]. Recently, a novel hybrid individual-machine-EAC method (IMEAC) was proposed [15]–[17]. The effectiveness of the method is further explained through the individual-machine-transient-energy (IMTE) [18]. The precise modeling of the individual-machine potential energy surface (IMPES) is also established [19]. The thinking behind NEC greatly inspires modern individual-machine transient stability studies.

Originally, power system transient stability is a trajectory stability problem [15]. However, historical global works and recent individual-machine studies indicate that the precise transient energy conversion inside each machine, the modeling of the IMPES, and the equivalence between transient energy conversion and the EAC inside each machine cannot be treated as a coincidence. Instead, all these phenomena reveal that the power system transient stability should be explained through Newtonian mechanics. In fact, Newtonian-like models, such as the Kuramoto-like model [20] and the ball-on-concave-surface model [21], were developed to assist the transient stability evaluation. However, these models were generally equivalent or abstract, and thus, they cannot be used to establish strict mappings between the Newtonian-mechanical model and the multimachine power system model. Against this background, the strict mappings between the individual machine transient stability model and the Newtonian mechanical model become of value, because they may essentially establish the theoretical foundation of the individual-machine transient stability from the perspective of Newtonian mechanics.

B. SCOPE AND CONTRIBUTION OF THE PAPER
Following Refs. [18], [19], this paper is the theoretical exploration of the individual-machine transient stability from the perspective of Newtonian mechanics. In this paper, the original Newtonian system is formed by a concrete ball and the Earth with variant gravity. The Newtonian energy conversion (NEC) inside the system is precisely characterized by using the occurrence of the residual KE. The EAC can be considered a reflection of the Newtonian work and it is identical to the NEC. Based on these features, the stability characterizations of the Newtonian system are given. Furthermore, a generalized Newtonian system with multiple balls is developed. The generalized Newtonian system can be decomposed into multiple two-ball-based subsystems. The force of each subsystem reflects the complicated interactions among all balls in the entire generalized system. Most importantly, the stability of each subsystem is characterized independently in parallel through its corresponding NEC after decomposition. Finally, strict mappings between the Newtonian system stability and individual-machine transient stability are established. Based on all these strict mappings, the authors state that the theoretical foundation of individual-machine thinking should be Newtonian mechanics.

The contributions of this paper are summarized as follows:

(i) The precise modeling of the original Newtonian system with two balls is established. This modeling explains the mechanisms of the NEC and EAC through Newtonian mechanics.

(ii) The precise modeling of the generalized Newtonian system with multiple balls is established. The decomposition of the system explains the mechanisms of independent parallel stability characterization.

(iii) Strict mappings between individual-machine transient stability and Newtonian system stability are discovered. Newtonian mechanics is finally set as the theoretical foundation of individual machine transient stability.

The remainder of the paper is organized as follows. In Section II, the modeling of the original Newtonian system is given, and NEC is analyzed. In Section III, the original Newtonian system is extended to a generalized Newtonian system with multiple balls. In Section IV, strict mappings between Newtonian system stability and individual-machine transient stability are analyzed. In Section V, simulation cases are provided to show the NEC inside each machine. In Section VI, further discussions about the Newtonian system are provided. Conclusions are given in Section VII.

The generalized Newtonian system that is developed in this paper will show extremely strict mappings with the multimachine power system. However, the authors emphasize that the generalized Newtonian system is not used to assist transient stability analysis. This is because the individual-machine transient stability analysis is fully based on the IMEAC [15]–[17]. In fact, this Newtonian-mechanical system is only used to validate that the theoretical foundation of the individual-machine transient stability is Newtonian mechanics.

The fault types for the transient stability analysis in this paper are defined the same as those in Refs. [15]–[19]. The test systems, i.e., TS-1 to TS-5, can be found in
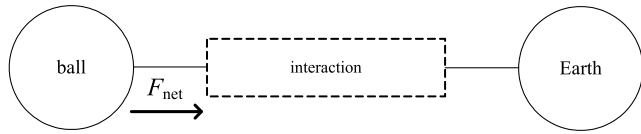
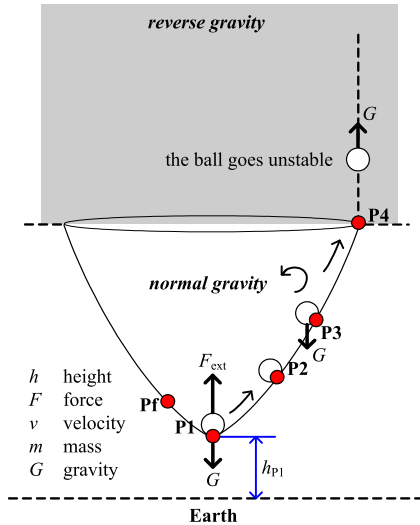**FIGURE 1.** Formation of the original Newtonian system.

FIGURE 2. Structure of the original Newtonian system.

Refs. [15]–[19]. All faults are three-phase short-circuit faults, which occur at 0 s. The fault is cleared without line switching.

II. ORIGINAL NEWTONIAN SYSTEM

A. NEWTONIAN ENERGY CONVERSION

This section first focuses on the mechanism of the original Newtonian system with two balls.

The original Newtonian system is formed by two balls, i.e., a concrete ball and an infinitely large Earth. The two balls interact through the internal force between them. A demonstration of the original Newtonian system is shown in Fig. 1.

In the original Newtonian system, each ball has its own equation of motion. The motion of the ball is given as

$$\begin{cases} \dfrac{dh}{dt} = v \\ m\dfrac{dv}{dt} = F_{\text{net}} \end{cases} \tag{1}$$

In Eq. (1), F_{net} and h are the "net force" and the altitude of the ball, respectively. Other parameters are shown in Fig. 2.

In the original Newtonian system, the Earth remains stationary ($m_{\text{earth}} = \infty$, $h_{\text{Earth}} = 0$). The equation of motion of the Earth is given as

$$\begin{cases} \dfrac{dh_{\text{Earth}}}{dt} = v_{\text{Earth}} = 0 \\ \dfrac{dv_{\text{Earth}}}{dt} = \dfrac{F_{\text{Earth}}}{m_{\text{Earth}}} = 0 \end{cases} \tag{2}$$

Following Eq. (2), the stationary Earth is set as the "motion reference" of the system.

Based on Eqs. (1) and (2), the relative motion between the ball and Earth is given as

$$\begin{cases} \dfrac{d(h - h_{\text{Earth}})}{dt} = v - v_{\text{Earth}} = v \\ m\dfrac{d(v - v_{\text{Earth}})}{dt} = F_{\text{net}} - \dfrac{m}{m_{\text{Earth}}}F_{\text{Earth}} = F_{\text{net}} \end{cases} \tag{3}$$

Eq. (3) describes the separation between the ball and Earth inside the original Newtonian system. Since the Earth is stationary, the altitude (h) and the velocity (v), as in Eq. (1) also describe the relative motion between the ball and Earth. The altitude is named the "trajectory" of the ball by using the Earth as the motion reference.

In the following analysis, the dynamic behavior of the Newtonian system is visually depicted through a ball rolling inside a basin. The structure of the original Newtonian system is shown in Fig. 2. The basin in the system depicts the position of the ball. Note that the original Newtonian system is defined as a "gravity-variant" system. That is, the gravitational field is assumed to reverse once the ball goes over the edge of the basin. This is different from the constant gravity environment. In addition, the "velocity" in this paper specifies the velocity along the altitude in the system.

From Fig. 2, at first, the ball remains stationary at the bottom of the basin (P1). At t_0, an "external force" imposes on the ball. This external force is given as

$$F_{\text{ext}} = F_{\text{acc}} + G \tag{4}$$

Following Eq. (4), the net force at P1 becomes F_{acc}. F_{ext} overcomes gravity and causes the ball to accelerate.

Assume the energy reference point of the system is set as P1. Following the Newtonian kinetic energy theorem, the acceleration of the ball from P1 to P2 is calculated as

$$\int_{h^{(\text{P1})}}^{h^{(\text{P2})}} F_{\text{acc}}dh = \frac{1}{2}mv^{(\text{P2})2} - 0 \tag{5}$$

At P2, the total energy of the ball is calculated as

$$V^{(\text{P2})} = \frac{1}{2}mv^{(\text{P2})2} + \int_{h^{(\text{P1})}}^{h^{(\text{P2})}} Gdh \tag{6}$$

From Eq. (6), the total energy comprises two components, i.e., the KE and PE. Since the total energy increases from zero to $V^{(\text{P2})}$ at P2, the period from P1 to P2 is named the "disturbance-on" period.

Once the ball reaches P2, the external force (F_{ext}) is cleared at the moment. Under this circumstance, the only force that imposes on the ball becomes the "internal force", i.e., gravity ($F_{\text{net}} = G$). Then, the ball starts decelerating with only gravity acting on it.

For the period after P2, one can obtain the following:

$$\frac{dV}{dt} = mv\frac{dv}{dt} + G\frac{dh}{dt} = 0 \tag{7}$$

Eq. (7) indicates that the total energy of the ball remains "conserved" after P2 because only the internal force, i.e., gravity, acts on the ball. The period after the disturbance clearing is named the "post-disturbance" period.

In the post-disturbance period, the maximum potential energy of the ball is calculated as

$$V_{PE}^{cr} = V_{PE}^{(P4)} = \int_{h^{(P1)}}^{h^{(P4)}} Gdh \qquad (8)$$

From Eq. (8), the ball reaches the edge of the basin at P4 with the maximum PE.

In the original Newtonian system, P4 is named the "dynamic liberation point" (DLP). From the energy conversion perspective, the condition that the ball goes through the DLP is given as

$$V^{(P2)} > V_{PE}^{cr} \qquad (9)$$

From Eq. (9), physically, the ball will escape from the basin once it accumulates very high KE at P2, and this amount of KE *cannot* be fully absorbed at the DLP.

Following Eq. (9), the energy conversion at the DLP is given as

$$V_{KE}^{RE} = V^{(P2)} - V_{PE}^{cr} = \frac{1}{2}mv^{(P2)2} - \Delta V_{PE} \qquad (10)$$

where

$$\Delta V_{PE} = V_{PE}^{cr} - V_{PE}^{(P2)} = \int_{h^{(P2)}}^{h^{(DLP)}} Gdh$$

In Eq. (10), the residual KE is of key value because it finally causes the ball to escape from the basin at the DLP.

Assume gravity becomes reversed once the ball goes through the DLP. Against this background, the internal force is given as

$$G = \begin{cases} mg & h \leq h^{(DLP)} \\ -mg & h > h^{(DLP)} \end{cases} \qquad (11)$$

Following Eq. (11), the DLP describes the point where the ball becomes unstable. Once the ball goes through the DLP, it starts accelerating again and separates from the Earth with reverse gravity, as shown in Fig. 2.

Compared with the unstable case, if the accumulated KE at P2 is low, this KE will be completely absorbed before reaching the DLP. Under this circumstance, the PE will also reach a maximum at P3. The energy conversion at P3 is given as

$$V_{KE}^{RE} = \frac{1}{2}mv^{(P2)2} - \Delta V_{PE} = 0 \qquad (12)$$

where

$$\Delta V_{PE} = V_{PE}^{(P3)} - V_{PE}^{(P2)} = \int_{h^{(P2)}}^{h^{(P3)}} Gdh$$

Following Eq. (12), the residual KE is completely exhausted at P3, and thus, the ball inflects back. P3 is named the "dynamic stationary point" (DSP). It represents the point where the ball maintains stable.

From the analysis above, clear energy conversion between KE and PE can be found in the original Newtonian system. The characteristics of this energy conversion are summarized as follows:

(i) The total energy keeps increasing during the disturbance-on period, and it remains conservative during the post-disturbance period.

(ii) The PE may reach a maximum during the post-disturbance period.

In this paper, this energy conversion is named the "Newtonian energy conversion" (NEC). In particular, for (ii), the occurrence of the maximum PE along time horizon is analyzed as below.

1) UNSTABLE CASE

dh is always positive during the post-disturbance period. However, because G changes from positive to negative when the ball goes through the DLP, the integral of Gdh is first positive and then becomes negative. Therefore, the PE will reach a maximum when the ball becomes unstable.

2) STABLE CASE

G is always positive during the post-disturbance period. However, because dh changes from positive to negative when the ball inflects back at the DSP, the integral of Gdh is first positive and then becomes negative. Therefore, the PE will also reach a maximum when the ball remains stable.

From the analysis above, in the original Newtonian system, the PE of the ball may reach a maximum at the DLP or DSP regardless of whether the system becomes unstable. The DLP or DSP is also the "maximum potential energy point" (MPP) of the system. However, if we observe only the variation in the PE of the ball, one problem is that we *cannot* confirm whether the MPP is a DSP or DLP because the PE reaches a maximum at the two points. Against this background, the stability of the system *cannot* be evaluated only through the variance in the PE. To solve this problem, the residual KE of the ball at the MPP should be used as the stability characterization of the system.

B. RESIDUAL KINETIC ENERGY

Following Eqs. (10) and (12), the residual KE can be given in a general form:

$$V_{KE}^{RE} = V_{KE}^{(P2)} - \Delta V_{PE} \qquad (13)$$

where

$$V_{KE}^{(P2)} = \frac{1}{2}mv^{(P2)2}$$

$$\Delta V_{PE} = \int_{h^{(P1)}}^{h^{MPP}} Gdh - \int_{h^{(P1)}}^{h^{(P2)}} Gdh = \int_{h^{(P2)}}^{h^{MPP}} Gdh$$

In Eq. (13), V_{KE}^{RE} is the residual KE at the MPP. The ball will become unstable if V_{KE}^{RE} is positive at the MPP (the MPP would be the DLP), and the ball will remain stable if V_{KE}^{RE} is zero at the MPP (the MPP would be the DSP).

Based on NEC, the stability characterization of the system is summarized below.

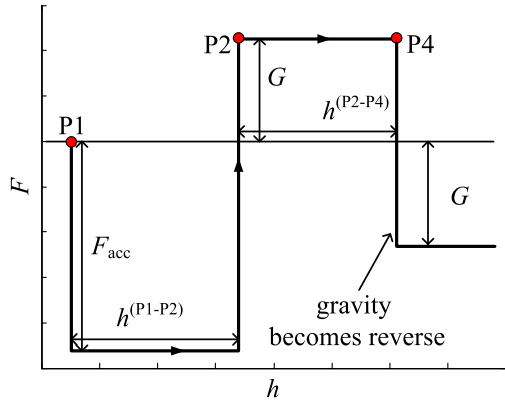*The ball will go unstable if residual KE occurs at the MPP.*

FIGURE 3. EAC of a ball becoming unstable.

This statement reveals that the NEC is "perfect" because the stability state of the ball is precisely identified through the occurrence of residual KE at the MPP.

C. NEWTONIAN WORK AND EQUAL AREA CRITERION

If we observe the NEC in the F-h space rather than the t-V space, the "areas" can be found in this space. For the unstable case, the motion of the unstable ball is shown in Fig. 3.

From Fig. 3, the area from P1 to P2 and that from P2 to P4 form the "acceleration area" and the "deceleration area", respectively. Observing this phenomenon from the perspective of Newtonian mechanics, this "area" is identical to the "Newtonian work". In particular, the work on the ball from P1 to P2 is $F_{\text{acc}}h^{(\text{P1}-\text{P2})}$ (the net force is F_{acc} during the disturbance-on period), while the work from P2 to P4 is $Gh^{(\text{P2}-\text{P4})}$ (the net force is G during the post-disturbance period).

From the analysis above, the NEC can also be described in an "equal-area-criterion" (EAC) manner. Based on Newtonian mechanics, the following theorem is given.

Theorem: The NEC is identical to the EAC in the original Newtonian system.

Proof: For the case in which the ball becomes unstable, following Eq. (5), the acceleration area from P1 to P2 is calculated as

$$A_{\text{acc}} = \int_{h^{(\text{P1})}}^{h^{(\text{P2})}} F_{\text{acc}}dh = \frac{1}{2}mv^{(\text{P2})2} \tag{14}$$

The deceleration area from P2 to DLP is expressed as

$$A_{\text{dec}} = \int_{h^{(\text{P2})}}^{h^{(\text{DLP})}} Gdh = \int_{h^{(\text{P1})}}^{h^{(\text{DLP})}} Gdh - \int_{h^{(\text{P1})}}^{h^{(\text{P2})}} Gdh \tag{15}$$

Following Eqs. (13-15), one can obtain the following equation:

$$V_{KE}^{RE} = A_{\text{acc}} - A_{\text{dec}} \tag{16}$$

Eq. (16) reveals that the NEC and EAC are identical. Thus, the theorem holds.

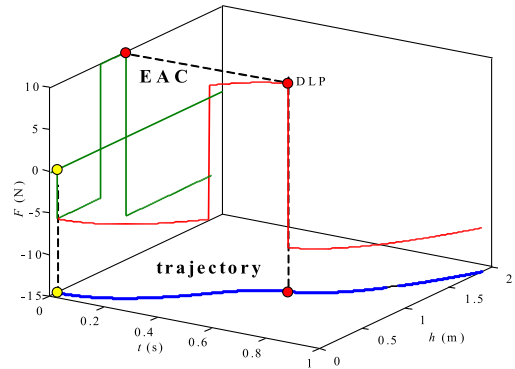Based on the EAC, the stability characterization of the system is summarized below.

FIGURE 4. Three-dimensional EAC in the original Newtonian system.

The ball will become unstable if the acceleration area is larger than the deceleration area.

Additionally, based on the EAC, the critical state for the ball to maintain stability should be calculated as

$$\int_{h^{(\text{P1})}}^{h^{cr}} F_{\text{acc}}dh = \int_{h^{cr}}^{h^{(\text{P4})}} Gdh \tag{17}$$

In Eq. (17), h^{cr} describes the critical clearing point of the external force. Once the altitude of the disturbance clearing point ($h^{(\text{P2})}$) is higher than h^{cr}, the acceleration area will be larger than the deceleration area, and the ball becomes unstable.

To demonstrate the relationship between the EAC and the trajectory of the ball, a 3-dimensional EAC in t-h-F space is proposed, as shown in Fig. 4.

From Fig. 4, the 3-dimensional EAC is obtained from the equation of motion of the ball. Against this background, the trajectory and EAC of the ball can be considered the two projections of the three-dimensional EAC in t-h space and h-F space, respectively. The EAC in the h-F space is just a "characterization window" to measure the trajectory stability of the ball.

D. FREE SETTING OF THE ENERGY REFERENCE POINT

In classic Newtonian mechanics, as analyzed in Section A, the energy reference point of the PE is always set as P1 by default. In fact, a distinctive characteristic of the original Newtonian system is that the NEC is independent of the energy reference point. In the following analysis, the energy reference point will be set as a random point (Pf) along the trajectory of the ball, regardless of whether Pf occurs before or after the disturbance clearing.

Using the randomly selected Pf, the TE at the fault clearing point is calculated as

$$V^{(\text{P2})} = \frac{1}{2}mv^{(\text{P2})2} + \int_{h^{(\text{Pf})}}^{h^{(\text{P2})}} Gdh \tag{18}$$

The maximum PE that occurs at the DLP is given as

$$V_{PE}^{DLP} = \int_{h^{(\text{Pf})}}^{h^{(\text{DLP})}} Gdh \tag{19}$$

Parameters	Value
m	1.000 kg
G	9.800 m/s^2
F_{ext}	16.000 N
h_{P1}	0.100 m
h_{DLP}	0.897 m

Based on Eqs. (18) and (19), we have

$$
\begin{aligned}
V_{KE}^{RE} &= V^{(\text{P2})} - V_{PE}^{DLP} \\
&= V_{KE}^{(\text{P2})} - \Delta V_{PE} = A_{\text{acc}} - A_{\text{dec}}
\end{aligned} \tag{20}
$$

Eq. (20) indicates that the residual KE is determined only by the acceleration area and the deceleration area, which is completely independent of the setting of the energy reference point.

The free setting of the energy reference point shows that it is the "energy conversion" (also the Newtonian work) rather than the "energy" that finally determines the stability of the ball. This finding also validates the equivalence between the NEC and EAC, as analyzed in Section C.

E. STABILITY CHARACTERIZATIONS OF THE ORIGINAL NEWTONIAN SYSTEM

Following the NEC and EAC as analyzed in Sections A and C, the stability characterizations of the original Newtonian system are given below.

(i) From the perspective of NEC, the system is evaluated to be unstable if residual KE occurs at the MPP.

(ii) From the perspective of the EAC, the system is evaluated to become unstable if the acceleration area is larger than the deceleration area.

Note that (i) and (ii) are identical.

A tutorial example is given to demonstrate the NEC inside the original Newtonian system. The parameters are shown in Table 1. The external force occurs at 0.000 s and is cleared at 0.400 s. The energy reference point is set as P1 in this case.

Following Newtonian mechanics, the motion of the ball during the disturbance-on period ($t \leq t_c$) is given as

$$
\begin{cases}
v_t = v_0 + at \\
h = h_{\text{P1}} + \dfrac{1}{2}at^2
\end{cases} \tag{21}
$$

With 0.400 s acceleration, the ball reaches P2, and the height becomes 0.596 m. At this moment, the velocity of the ball is 2.480 m/s.

Then, the external force is cleared, and the ball starts decelerating until it reaches the DLP. The motion of the ball during the post-disturbance period ($t_c < t < t_{DLP}$) is given as

$$
\begin{cases}
v_t = v_{\text{P2}} - g(t - t_c) \\
h = h_{\text{P2}} + v_{\text{P2}}(t - t_c) - \dfrac{1}{2}g(t - t_c)^2
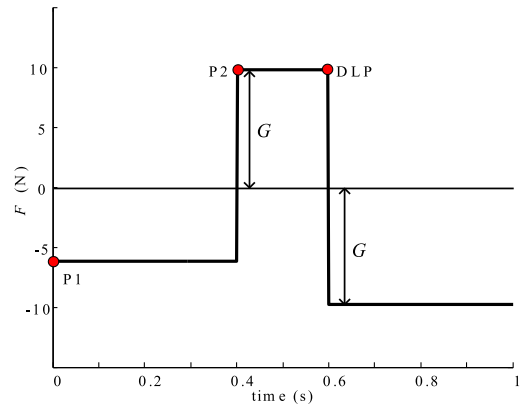\end{cases} \tag{22}
$$

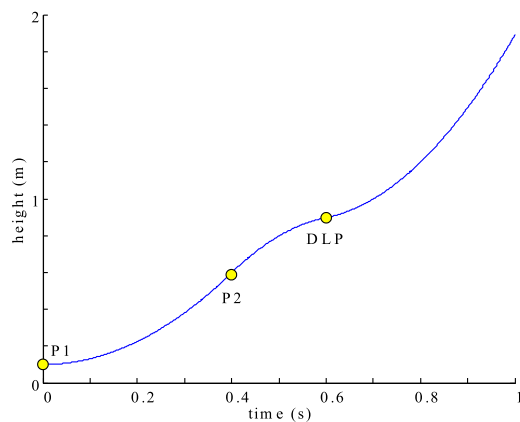**FIGURE 5.** Net force along the time horizon.
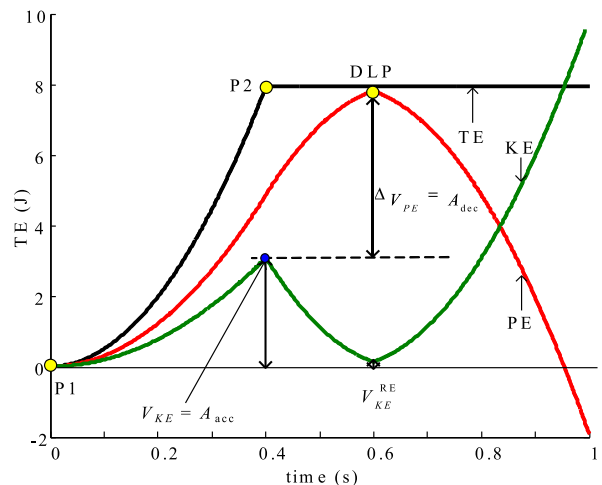

FIGURE 6. Trajectory of the ball.

FIGURE 7. NEC in the unstable original Newtonian system.

At 0.600 s, the ball reaches the DLP, and the altitude is 0.896 m. The velocity of the ball reaches 0.520 m/s.

Once the ball goes through the DLP, the gravity becomes reversed. The net force and trajectory of the ball along time horizon are shown in Figs. 5 and 6, respectively. The NEC and EAC are shown in Figs. 7 and 8, respectively.
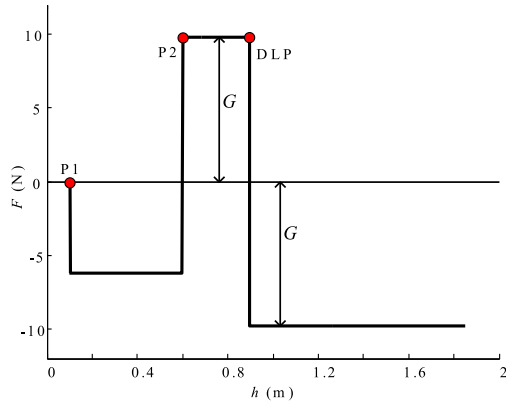
FIGURE 8. EAC in the unstable original Newtonian system.

Stability evaluations of the system are shown below

1) NEC ANGLE
From Fig. 7, during the post-disturbance period, the PE reaches a maximum at the DLP with residual KE (0.137 J). Furthermore, this residual KE forces the ball to fall into the reverse gravitational field, and thus, the ball starts accelerating again. Against this background, the KE of the ball becomes positive infinite. The altitude of the ball also becomes infinite along the time horizon, as shown in Fig. 6. The ball finally becomes unstable.

2) EAC ANGLE
From Fig. 8, the acceleration area, i.e., the work from P1 to P2, is 3.078 J, while the deceleration area, i.e., the work from P2 to the DLP, is 2.941 J. The acceleration area and the deceleration area are identical to the V_{KE} at P2 and ΔV_{PE}, respectively. Since the acceleration area is larger than the deceleration area, the ball becomes unstable. Note that the difference between the two areas is just the residual KE (0.137 J).

This simulation case visually demonstrates the equivalence between the NEC and EAC in the original Newtonian system.

F. CONTINUOUS VARIANCE IN GRAVITY
In the predefined original Newtonian system, a sudden change in gravity will occur once the ball goes through the DLP, as shown in Fig. 5. In fact, the reverse procedure of gravity can also be depicted in a "continuous" manner.

Assume the gravity of the ball is modified as

$$G = G(h) \quad (23)$$

From Eq. (23), gravity after disturbance clearing is decided by the "continuous" trajectory of the ball. Against this background, the variance in gravity will also become "continuous" without any sudden changes.

Taking the case in Section E as an example, assume gravity is given as

$$G = \begin{cases} mg & h \leq h^{(P2)} \\ mg\cos[k(h - h_{P2})] & h > h^{(P2)} \end{cases} \quad (24)$$
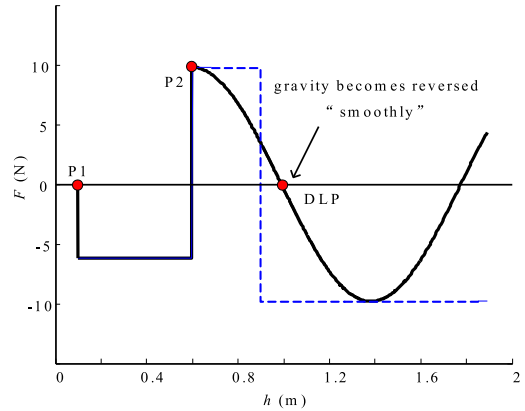

FIGURE 9. EAC in the unstable system.

Following Eq. (24), the EAC with the continuous variance in gravity is shown in Fig. 9. k is set as 4 for this case.

From Fig. 9, after the disturbance clearing, the "value" of gravity decreases with increasing h until it reaches zero. After that, the "direction" of gravity smoothly reverses, and its value also gradually increases with increasing h. The variance in gravity becomes continuous without any sudden changes.

Following the continuous variance in gravity, the occurrence of the DLP can be regiven as

$$G_{\mathrm{DLP}} = 0 \quad (25)$$

Mathematically, the occurrence of the DSP is given as

$$v_{\mathrm{DSP}} = 0 \quad (26)$$

From Eqs. (25) and (26), the occurrences of the DLP and DSP are described by gravity and velocity reaching zero, respectively. Eq. (25) also indicates that the DLP can be obtained through the occurrence of "zero gravity".

G. ADVANTAGES OF NEC
Following the analysis in Sections B and C, the characteristics of the MPP are summarized as follows:

(i) From the perspective of NEC, the DLP is the MPP with positive residual KE, while the DSP is the MPP with zero residual KE.

(ii) From the perspective of the EAC, the DLP is the point where gravity reverses, while the DSP is the point where gravity remains normal.

Following (i) and (ii), MPP is just the reflection of NEC by using the stability boundary point, and thus it can also be used as the trajectory description of the ball. The depiction of the trajectory by using the MPP is given as follows:

(i) The DLP is the point where the trajectory starts separating ($\mathrm{d}^2h/\mathrm{d}t^2 = G_{\mathrm{DLP}} = 0$).

(ii) The DSP is the point where the trajectory inflects back ($\mathrm{d}h/\mathrm{d}t = v_{\mathrm{DSP}} = 0$).

Based on the analysis above, the two advantages of the NEC are summarized as follows:

Stability-characterization advantage: The trajectory stability of the ball is characterized precisely at MPP.

Trajectory-depiction advantage: The trajectory variance of the ball is depicted clearly at MPP.

Based on the two advantages, if a physical system shows strict mappings with the original Newtonian system, it is clear that the two advantages will naturally be inherited in this physical system. In the following paper, the original Newtonian system will be extended to a more complicated multi-ball case.

III. GENERALIZED NEWTONIAN SYSTEM

A. SYSTEM MODELING

Following the previous definition of the original Newtonian system, the generalized Newtonian system is formed by multiple balls and the Earth. Note that each ball still uses the stationary Earth as the motion reference in the generalized system.

The equation of motion of the ith ball in the system is given as

$$\begin{cases} \dfrac{dh_i}{dt} = \dfrac{d(h_i - h_{\text{Earth}})}{dt} = v_i \\ m_i \dfrac{dv_i}{dt} = m_i \dfrac{d(v_i - v_{\text{Earth}})}{dt} = F_{\text{net},i} \end{cases} \quad (27)$$

In Eq. (27), $F_{\text{net},i}$ is the "net force" that imposes on the ith ball. h_i represents the altitude between the ith ball and the Earth.

We go a step further. Assume that $F_{\text{net},i}$ in the ith subsystem is affected by the trajectories of "all" balls in the system. In this way, $F_{\text{net},i}$ is given as

$$F_{\text{net},i} = F_{\text{net},i}(\boldsymbol{h}) \quad (28)$$

In Eq. (28), $\boldsymbol{h}$ is defined as the "system trajectory" that is formed by the trajectories of all the balls in the system. $F_{\text{net},i}$ reflects the effect on the ith ball from all balls (including the ith ball itself) in the system.

Based on the equation of motion of the ball as in Eqs. (27) and (28), the Newtonian energy of the ith ball is defined as

$$V_i = \frac{1}{2} m_i v_i^2 + \int_{h_i^{(P1)}}^{h_i} G_i(\boldsymbol{h}) dh_i \quad (29)$$

In Eq. (29), the energy reference point of the ith ball is set as P1. The energy conversion reflects the relative motion of the ball with respect to the Earth.

From the analysis above, the generalized Newtonian system is also a "gravity-variant" system. Since the trajectory of each ball (h_i) is continuous, the system trajectory is also continuous, and thus, the variance in the net force on each ball ($F_{\text{net},i}(\boldsymbol{h})$) will be continuous during the post-disturbance period. This situation fully indicates that the gravity of each ball in the generalized Newtonian system will become reversed smoothly without any sudden changes.

The formation of the generalized Newtonian system is shown in Fig. 10. Note again that the Earth is also a component of the system.
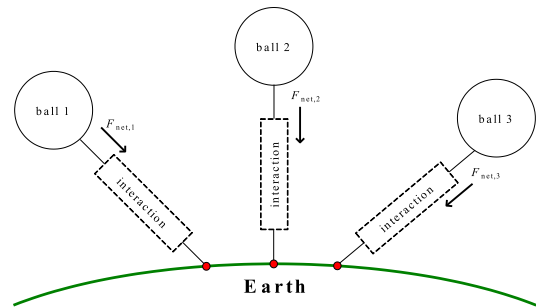

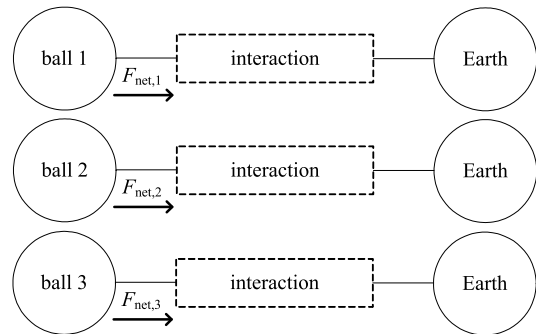**FIGURE 10.** Formation of the generalized Newtonian system.

FIGURE 11. Formation of the decomposed subsystem.

From Fig. 10, the characteristics of the generalized system are given as follows:

(i) $F_{\text{net},i}$ on each ball is affected by the system trajectory (h), and thus $F_{\text{net},i}$ varies continuously along the system trajectory, as in Eq. (28).

(ii) The variance in $F_{\text{net},i}$ will further change the trajectory of the ith ball (h_i), as in Eq. (27).

(iii) Each $F_{\text{net},i}$ is unique and different, although it corresponds to the same system trajectory ($\boldsymbol{h}$).

(iv) h_i of each ball is unique and different because each $F_{\text{net},i}$ is different.

(i) to (iv) indicate that $F_{\text{net},i}$ and h_i "cause and effect" each other.

Considering that each ball is a fundamental component in the generalized Newtonian system, the stability state of the entire system is naturally decided by the stability state of each ball. Therefore, the stability principle of the system can be defined as follows:

(I) The generalized Newtonian system can be considered to be stable if all balls are stable.

(II) The generalized Newtonian system can be considered to be unstable as long as any ball is found to become unstable.

The two principles substantially illustrate the stability mechanism of the generalized Newtonian system. In particular, Principle II reveals that the entire generalized system becoming unstable can be decided by any one ball becoming unstable.

B. INDEPENDENT PARALLEL STABILITY CHARACTERIZATION

Following the analysis in Section A, crucial characteristics of the generalized Newtonian system are depicted as follows.
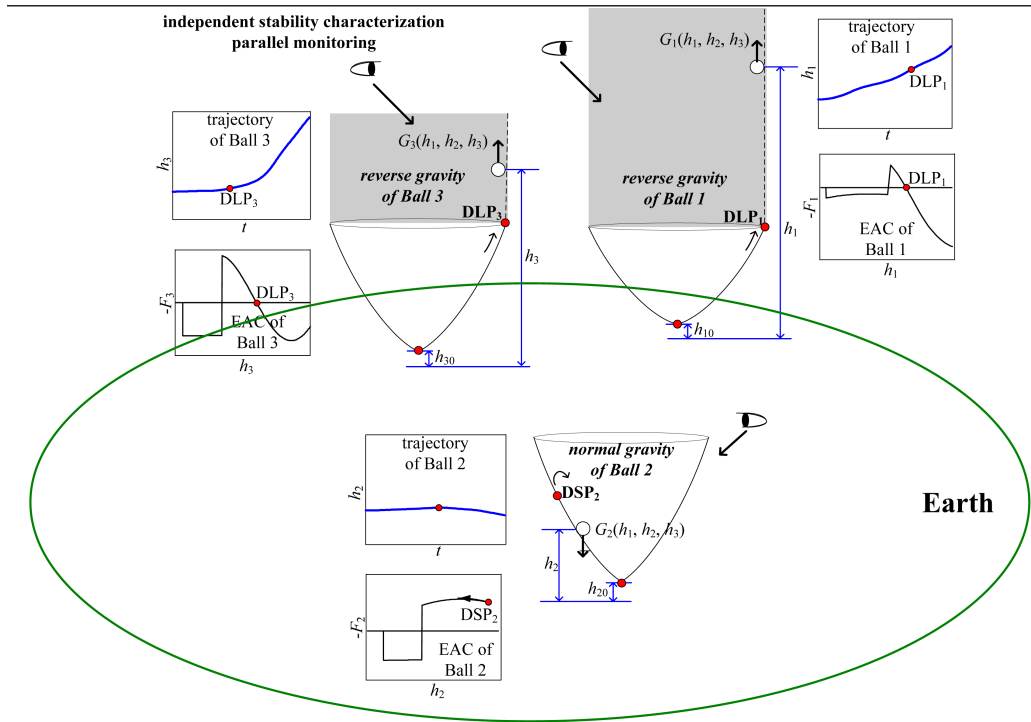
FIGURE 12. Independent parallel stability characterization of the generalized Newtonian system.

(i) The Earth is set to the same motion reference of each ball in the generalized system.

(ii) $F_{net,i}$ is the "one and only" force that acts on the ith ball, although it is determined through the trajectories of all balls in the system ($\boldsymbol{h}$).

The two characteristics of the generalized Newtonian system strongly indicate that the entire system can be decomposed into multiple two-ball-based subsystems. Each subsystem is formed by an individual ball and the Earth with the net force on the ball. The structure of each subsystem is also completely the same as that of the original Newtonian system.

The decomposition of the generalized Newtonian system is shown in Fig. 11.

Following the analysis of the original Newtonian system as analyzed in Section II, by using the Earth as the motion reference, the formation of each sub-system after decomposition fully indicates the following

The stability of each ball can be characterized independently, although all balls interact with each other.

The NEC inside each subsystem is unique and different because the net force inside each ball is different.

This independence after decomposition further ensures the following attribute.

The stability of each ball after decomposition can be monitored in parallel.

Essentially, the "independent & parallel" stability characterization" can be considered the key feature of the stability characterizations of a generalized Newtonian system. Following the NEC inside each subsystem, the stability principle of

the generalized system in Section A can also be redefined in an NEC manner, as given below:

(I) The generalized Newtonian system can be considered stable if the residual KE of each ball is strictly zero at its MPP.

(II) The generalized Newtonian system can be considered to become unstable as long as the residual KE of any ball occurs at its MPP.

Based on the advantages of NEC as analyzed in Section II G, one can naturally obtain the following attributes.

The stability of each ball is characterized precisely at its corresponding MPP.

The trajectory of each ball is depicted clearly at its corresponding MPP.

A demonstration of the independent parallel stability characterization is shown in Fig. 12.

From Fig. 12, three subsystems are formed after decomposition. All these subsystems have the same motion reference, i.e., the Earth. The net force on each ball ($F_{net,i}(\boldsymbol{h})$) is unique and different, and thus, the NEC of each ball is unique and different. The stability of each ball is characterized independently in parallel through its corresponding NEC. The MPP (DLP or DSP) of each ball occurs one after another along the time horizon. According to the advantages of the NEC as analyzed in Section II G, the stability of each ball is characterized precisely at its MPP, and the trajectory of each ball is depicted clearly at its MPP. In the end, the stability of the entire system is characterized through the stability of each ball, according to the stability principle.
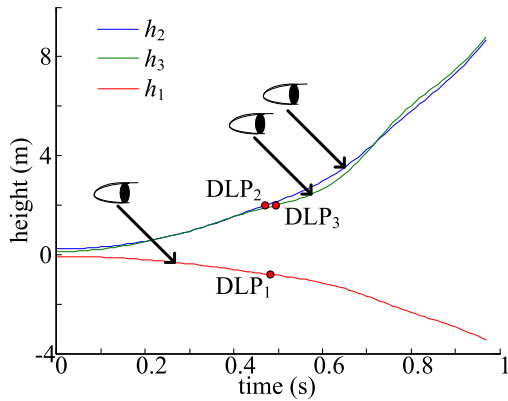
FIGURE 13. Parallel monitoring.

C. A TUTORIAL EXAMPLE

A tutorial example is given below to demonstrate the NEC inside the generalized Newtonian system. In this case, the generalized system is formed by three balls and the Earth. The net force of each ball follows the structure of f_i as given in the TS-4 test bed [19].

The net force of each ball is given as

$$F_{\text{net},i} = f_i(\boldsymbol{h}) \tag{30}$$

where

$$f_i = P_{mi} - P_{ei} - \frac{m_i}{m_T} \sum_{i=1}^{n} (P_{mi} - P_{ei}(\boldsymbol{h}))$$

$$m_T = \sum_{i=1}^{n} m_i$$

In Eq. (30), f_i is computed according to the structures of the power system during the fault-on period and postfault period, as given in Ref. [19]. Note that f_i can also be defined in other forms.

Assume the disturbance is set as [TS-4, bus-1, 0.40 s]. After decomposition, the generalized system becomes three subsystems, and each subsystem is formed by a ball and the Earth.

The system trajectory obtained by using the Earth as the motion reference is shown in Fig. 13. The trajectory (altitude) and EAC of each ball are shown in Figs. 14 and 15, respectively.

From Figs. 14 and 15, after decomposition, the stability of each subsystem is characterized independently, and each subsystem is monitored in parallel. Since the $F_{\text{net},i}(\boldsymbol{h})$ of each ball is different, the NEC (and EAC) of each ball is unique and different. The gravity of each ball is reversed smoothly at its DLP when zero gravity occurs. Once the ball goes through its DLP, the ball falls in its reverse gravitational field and becomes unstable. The DLP of each ball occurs one after another, as shown in Fig. 13. The instability of each ball is characterized precisely at its DLP, and the trajectory separation of each ball is also depicted clearly at its DLP. Following the stability principle, the entire system is evaluated to become unstable once Ball 2 becomes unstable at DLP$_2$.
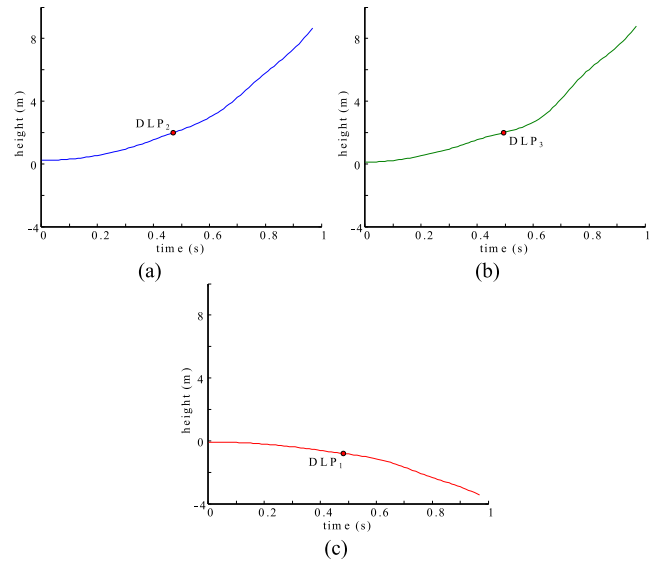

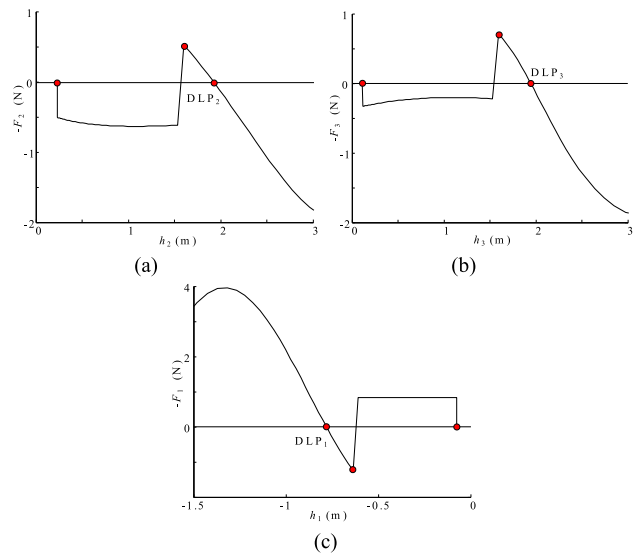**FIGURE 14.** Trajectory of each ball. (a) Ball 2. (b) Ball 3. (c) Ball 1.

FIGURE 15. Independent stability characterization. (a) EAC of Ball 2. (b) EAC of Ball 3. (c) EAC of Ball 1.

The example above visually demonstrates the independent parallel stability characterization of the generalized Newtonian system. In the following section, eight strict mappings between the Newtonian system stability and the individual-machine transient stability will be given. Based on all these mappings, we focus on the explanations of the mechanisms of the individual-machine transient stability from the perspective of Newtonian mechanics.

IV. MAPPINGS OF THE SYSTEM STABILITY
A. MAPPINGS BETWEEN THE ORIGINAL NEWTONIAN SYSTEM AND IVCS
1) MAPPING OF THE SYSTEM STRUCTURE (MAP-I)
Following the analysis in Ref. [15], for an n-machine system with rotor angle δ_i and inertia constant M_i, the motion of Machine i in the synchronous reference is governed by the
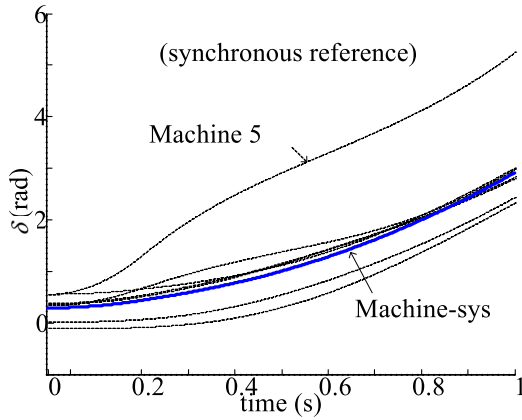
FIGURE 16. Motion of Machine-sys in the synchronous reference [TS-1, bus-34, 0.202 s].
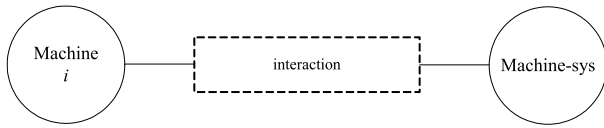

FIGURE 17. IVCS formed by machine *i* and Machine-sys.

differential equations

$$\begin{cases} \dfrac{d\delta_i}{dt} = \omega_i \\ M_i \dfrac{d\omega_i}{dt} = P_{mi} - P_{ei} \end{cases} \tag{31}$$

In Eq. (31), all the parameters are already given in Ref. [15].

The position of the center of inertia of the system (COI-SYS) is given as

$$\begin{cases} \delta_{\text{sys}} = \dfrac{1}{M_T} \sum_{i=1}^{n} M_i \delta_i \\ \omega_{\text{sys}} = \dfrac{1}{M_T} \sum_{i=1}^{n} M_i \omega_i \\ P_{\text{sys}} = \sum_{i=1}^{n} (P_{mi} - P_{ei}) \end{cases} \tag{32}$$

where $M_T = \sum_{i=1}^{n} M_i$

In Eq. (32), the COI-SYS can be considered an equivalent machine with its own equation of motion. Note that this motion represents the equivalent motion of all machines in the system. This equivalent machine is named Machine-sys. Notably, the motion of Machine-sys is given as

$$\begin{cases} \dfrac{d\delta_{\text{sys}}}{dt} = \omega_{\text{sys}} \\ M_T \dfrac{d\omega_{\text{sys}}}{dt} = P_{\text{sys}} \end{cases} \tag{33}$$

The trajectory of Machine-sys in the synchronous reference is shown in Fig. 16.

Because Machine *i* and Machine-sys are the two machines with interactions, an individual-machine-virtual-COI-SYS machine system (IVCS) can be formed, as shown in Fig. 17. Machine-sys is set as the motion reference of the IVCS.

TABLE 2. Structure-mapping between the Newtonian system and IVCS.

Original Newtonian system	IVCS
ball	Machine *i*
Earth	Machine-sys (COI-SYS)
Disturbance-on period	Fault-on period
Post-disturbance period	Postfault period
P1	SEP
P2	fault clearing point
P3	DSP
P4	DLP
G	$-f_i^{(PF)}$
F_{acc}	$f_i^{(F)}$
F_{ext}	$f_i^{(F)} - f_i^{(PF)}$
h	θ_i
v	$\tilde{\omega}_i$
m	M_i

The relative motion between Machine *i* and Machine-sys is given as

$$\begin{cases} \dfrac{d\theta_i}{dt} = \tilde{\omega}_i \\ M_i \dfrac{d\tilde{\omega}_i}{dt} = f_i \end{cases} \tag{34}$$

where

$$f_i = P_{mi} - P_{ei} - \dfrac{M_i}{M_T} P_{\text{sys}}$$
$$\theta_i = \delta_i - \delta_{\text{sys}}$$
$$\tilde{\omega}_i = \omega_i - \omega_{\text{sys}}$$

Eq. (34) gives the relative motion inside the IVCS.

Following the analysis in Section II A, strict mapping is found between the structure of the original Newtonian system and that of the IVCS. Detailed mapping is shown in Table 2.

From Table 2, the physically real machine and the equivalent Machine-sys in the IVCS can be considered the "ball" and the "Earth" in the original Newtonian system, respectively. The individual-machine trajectory (IMTR) of the machine in the COI-SYS reference also corresponds to the altitude of the ball in the original Newtonian system.

From the analysis above, the structure of the IVCS is fully in accordance with the structure of the original Newtonian system, as given in Section II A. Thus, strict mapping holds. Note that the structure-mapping essentially ensures all the following mappings.

2) MAPPING OF THE ENERGY DEFINITION (MAP-II)

The transient energy of an individual machine is defined as [18]

$$V_i = V_{KEi} + V_{PEi} \tag{35}$$

where

$$V_{KEi} = \dfrac{1}{2} M_i \tilde{\omega}_i^2$$
$$V_{PEi} = \int_{\theta_i^s}^{\theta_i} \left[-f_i^{(PF)}(\boldsymbol{\theta}) \right] d\theta_i$$

In Eq. (35), the components in V_i (M_i, $\tilde{\omega}_i$, f_i and θ_i) are the parameters of an individual machine. Therefore, V_i is the transient energy that is defined in a genuine individual-machine manner. The first and second terms on the right-hand side of Eq. (35) represent the individual-machine-kinetic-energy (IMKE) and the individual-machine-potential-energy (IMPE) of the machine, respectively.

From the analysis above, the definitions of the IMKE and IMPE are fully in accordance with the definition of the Newtonian energy, as given in Section II A. Thus, strict mapping holds.

3) MAPPING OF THE EQUIVALENCE BETWEEN ENERGY CONVERSION AND EAC (MAP-III)

Following the analysis in Refs. [15], [18], for an unstable critical machine, the acceleration area is calculated as

$$A_{ACCi} = \int_{\theta_i^s}^{\theta_i^c} f_i^{(F)} d\theta_i = \int_{\tilde{\omega}_i^s}^{\tilde{\omega}_i^c} M_i \tilde{\omega}_i d\tilde{\omega}_i = \frac{1}{2} M_i \tilde{\omega}_i^{c2} \quad (36)$$

The deceleration area is expressed as

$$A_{DECi} = \int_{\theta_i^c}^{\theta_i^{DLP}} \left[-f_i^{(PF)} \right] d\theta_i$$
$$= \int_{\theta_i^s}^{\theta_i^{DLP}} \left[-f_i^{(PF)} \right] d\theta_i - \int_{\theta_i^s}^{\theta_i^c} \left[-f_i^{(PF)} \right] d\theta_i \quad (37)$$

The residual IMKE is expressed in an EAC manner [18]

$$V_{KEi}^{RE} = A_{ACCi} - A_{DECi} \quad (38)$$

From the analysis above, the individual-machine transient energy conversion is fully identical to the IMEAC of the machine. This result is fully in accordance with the equivalence between the NEC and EAC, as given in Section II C. Thus, strict mapping holds.

4) MAPPING OF THE FREE SETTING OF THE ENERGY REFERENCE POINT (MAP-IV)

In Refs. [18], [19], the default energy reference point of IMPE is set as the prefault point θ^s. In fact, the energy reference point of IMPE can be set freely along the system trajectory, regardless of whether the point occurs before or after fault clearing.

Following Eq. (38), as analyzed in MAP-III, the residual IMKE is identical to the difference between the acceleration area and the deceleration area of the machine, which is independent of the settings of the energy reference point. This is fully in accordance with the free setting of the energy reference point in the original Newtonian system, as analyzed in Section II D. Thus, strict mapping holds.

5) MAPPING OF THE STABILITY CHARACTERIZATION (MAP-V)

Following the analysis in Refs. [15], [18], the stability characterizations of an individual machine are summarized below.

(i) From the perspective of transient energy conversion, a critical machine is evaluated to become unstable if the residual IMKE occurs at its IMPP.

(ii) From the perspective of the EAC, a critical machine is evaluated to become unstable if the acceleration area is larger than the deceleration area.

From the statements above, the stability characterizations of an individual machine are fully in accordance with the stability characterizations of the original Newtonian system, as given in Section II E. Thus, strict mapping holds.

In this section, strict mappings between IVCS and the original Newtonian system are given. In the following section, more mappings between the multimachine system and the generalized Newtonian system will be validated.

B. MAPPINGS BETWEEN THE GENERALIZED NEWTONIAN SYSTEM AND THE MULTI-MACHINE POWER SYSTEM

1) MAPPING OF THE SYSTEM STRUCTURE (MAP-VI)

We extend the transient characteristic of an individual machine into the multimachine case.

Under the COI-SYS reference, Machine-sys is set as the motion reference of all machines in a multimachine power system. Therefore, Machine-sys is identical to the "Earth" in the generalized Newtonian system, as analyzed in Section III A. Each machine shows correlations with Machine-sys through the net force (f_i) of the machine. This is completely in accordance with the structure of the generalized Newtonian system, as analyzed in Section III A. Thus, strict mapping holds.

2) MAPPING OF THE INDEPENDENT PARALLEL STABILITY CHARACTERIZATION (MAP-VII)

In the IVCS as analyzed in Ref. [15], each IVCS is formed by an individual machine and Machine-sys. Furthermore, because f_i describes the "one-and-only" force between the machine and Machine-sys, the stability of the IVCS can be characterized "independently". This fully reveals that the multimachine power system can be decomposed into each subsystem, i.e., the IVCS. Additionally, based on this independence, the transient behavior of each machine is monitored in "parallel". This is fully in accordance with the analysis in Section III B. Thus, strict mapping holds.

3) MAPPING OF THE STABILITY PRINCIPLE (MAP-VIII)

Following the analysis in Ref. [15], the unity principle of the multimachine power system is given as follows.

(i) The system can be considered stable if all critical machines are stable.

(ii) The system can be considered unstable as long as any unstable critical machine is found to become unstable.

From the statements above, the unity principle is fully in accordance with the stability principle of the generalized Newtonian system, as given Section III A. Thus, strict mapping holds.
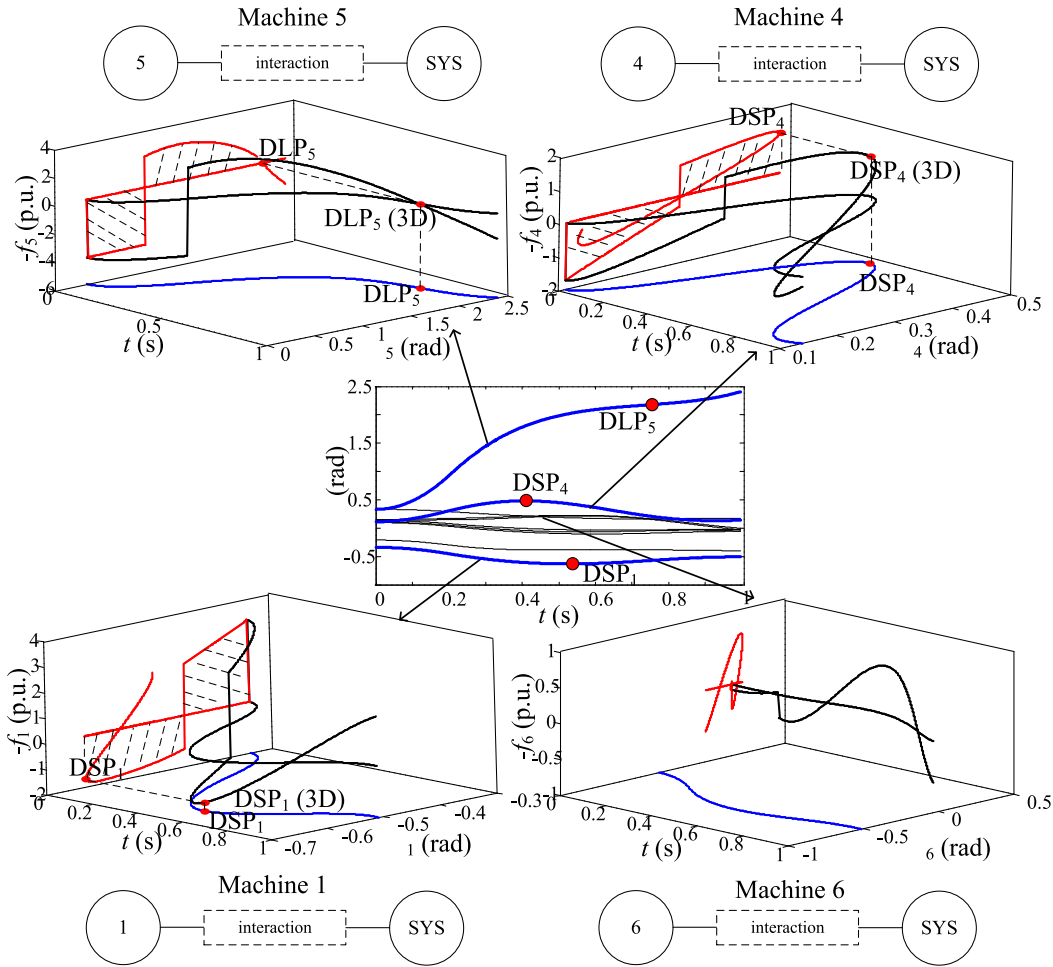
FIGURE 18. Mechanism of independent parallel stability characterization of the multimachine power system.

The mechanism of the independent parallel transient stability characterization of the multimachine power system is shown in Fig. 18.

From Figs. 12 and 18, strict mappings can be found between the generalized Newtonian system and multimachine power system. In particular, the multimachine power system is decomposed into multiple IVCSs. $f_i(\theta)$ of each machine fully reflects the complicated interactions among all machines in the system. Based on the 3DKC of the machine, the trajectory and Kimbark curve of the machine can be considered the two projections of the 3DKC of the machine in t-θ_i space and θ_i-f_i space, respectively. The stability of the machine is evaluated independently in parallel through its corresponding NEC. According to the advantages of the NEC as analyzed in Section II G, the stability of each machine is characterized precisely at the MPP, and the trajectory of each machine is depicted clearly at the MPP. Finally, the stability of the entire system is evaluated through the stability of each machine, according to the unity principle.

From all the mappings in the two sections above, the fundamental mechanism of the individual-machine transient stability can be explained effectively by using the Newtonian system.

V. CASE STUDY

A. NEC INSIDE ONE CRITICAL MACHINE
Two cases are given below to demonstrate the strict mappings between individual machine transient stability and original Newtonian system stability. Case-1 is [TS-1, bus-34, 0.219 s]. Case-2 is [TS-1, bus-34, 0.180 s]. In the following two cases, we only focus on the transient behaviors of Machine 5. Machine 5 becomes unstable in Case-1, while it remains stable in Case-2. IMTR$_5$ in the two cases is shown in Figs. 19 (a) and (b), respectively. The NEC and EAC of Machine 5 in the two cases are shown in Figs. 20 and 21, respectively.

From Figs. 20 and 21, following the mapping of the system structure and energy definition as analyzed in Section IV A (MAP-I and MAP-II), it is quite clear that the NEC and EAC can be established inside a critical machine (MAP-III). If residual IMKE$_5$ occurs at DLP$_5$, Machine 5 will become unstable with IMTR$_5$ going infinite in t-θ space, as shown in Fig. 19 (a). If residual IMKE$_5$ is strictly zero, Machine 5 will remain stable with IMTR$_5$ bounded in t-θ space, as shown in Fig. 19 (b). Therefore, the stability of Machine 5 is precisely depicted through its corresponding NEC and EAC (MAP-V).
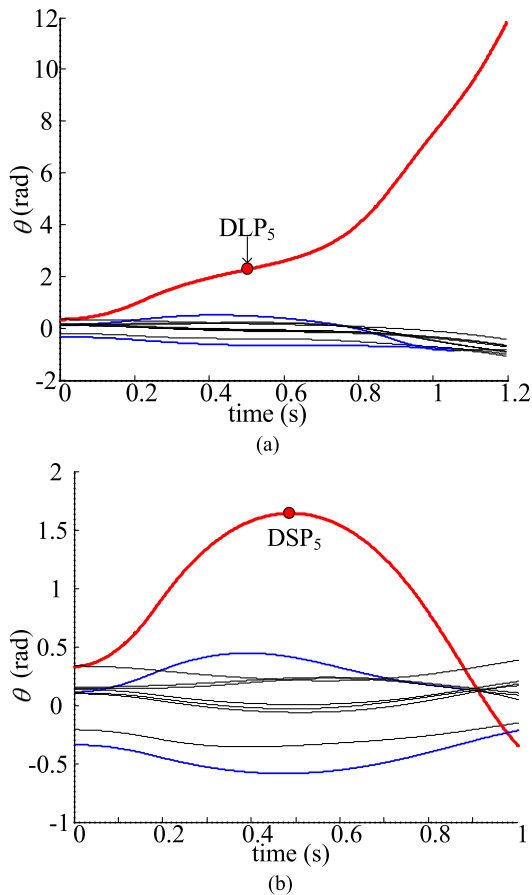
FIGURE 19. System trajectories. (a) Case-1: Machine 5 becomes unstable [TS-1, bus-34, 0.219 s]. (b) Case-2: Machine 5 maintains stable [TS-1, bus-34, 0.180 s].

Inside the $IVCS_5$ that is formed by Machine 5 and Machine-sys, the net force of the machine (f_5) is determined by the entire system trajectory (θ). Since the system trajectory is continuous along the time horizon, f_5 is also continuous during the postfault period, and thus, the "gravity" of the machine becomes reversed smoothly without any sudden changes, as shown in Fig. 20 (b). Against this background, DLP_5 occurs at the moment when f_5 reaches zero. Following the advantages of the NEC as analyzed in Section II G, the stability of the machine is characterized precisely at DLP_5, as in Figs. 20 and 21. The trajectory separation of the machine is also depicted clearly at DLP_5, as in Figs. 19 (a) and (b).

The simulation above fully shows that the IVCS is a typical original Newtonian system.

B. NEC INSIDE MULTIPE CRITICAL MACHINES

A simulation case is given to demonstrate the NEC inside a multimachine power system. The fault is [TS-1, bus-19, 0.230 s]. In this case, Machines 4, 5 and 1 are severely disturbed critical machines. Machine 5 becomes unstable, while Machines 4 and 1 remain stable. The system trajectory is shown in Fig. 22. The NEC inside each critical machine is
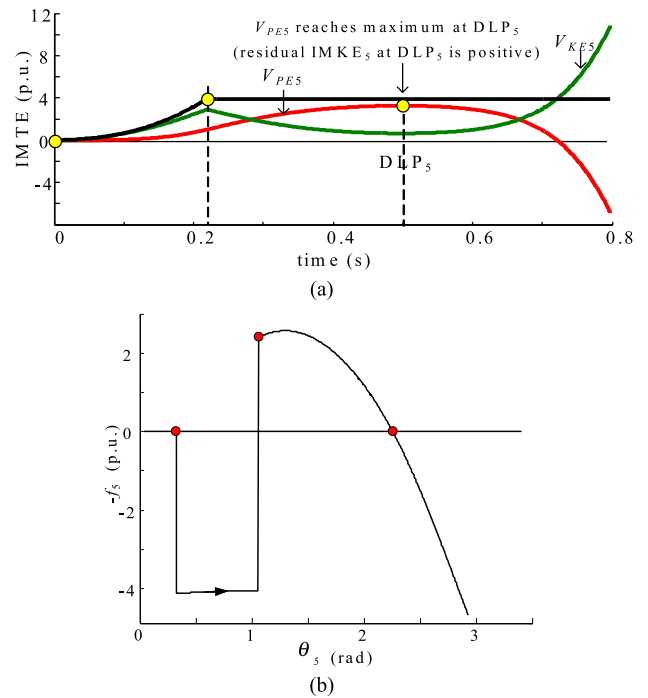

FIGURE 20. NEC and EAC inside Machine 5 in Case-1. (a) NEC. (b) EAC.
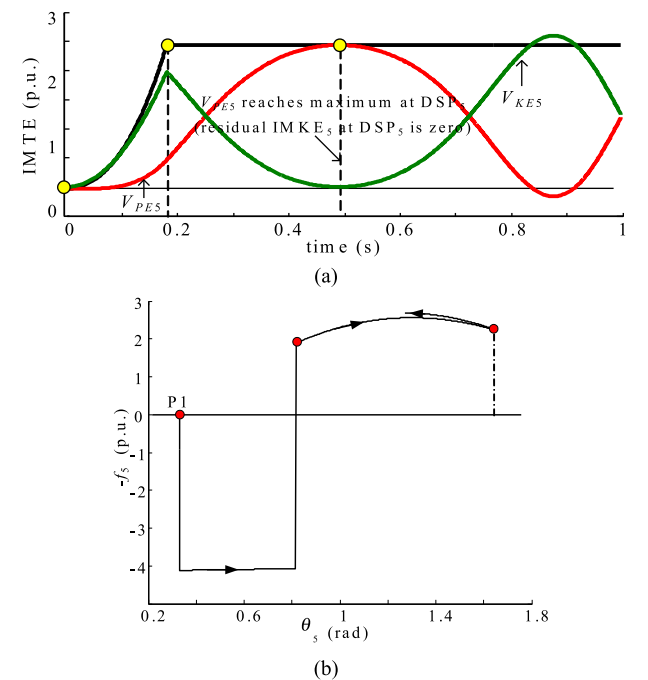

FIGURE 21. NEC and EAC inside Machine 5 in Case-2. (a) NEC. (b) EAC.

shown in Figs. 23 (a) to (c). In this case, the energy reference point of each IMPE is set as the prefault point θ^s as a default.

From Fig. 23, following the mapping of the system structure (MAP-VI), the multimachine power system is formed by ten subsystems, i.e., ten IVCSs. After decomposition, the stability of each machine is characterized independently in parallel (MAP-VII). The NEC of each machine is unique and different because f_i of each machine is different.
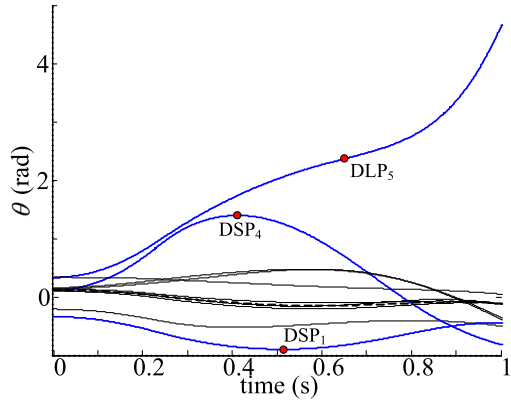
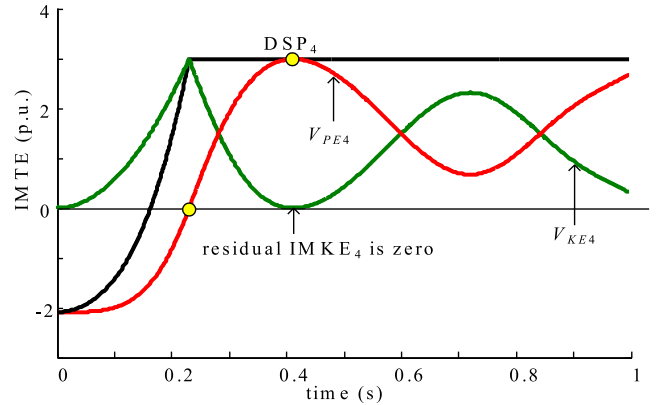**FIGURE 22.** System trajectory [TS-1, bus-19, 0.230 s].
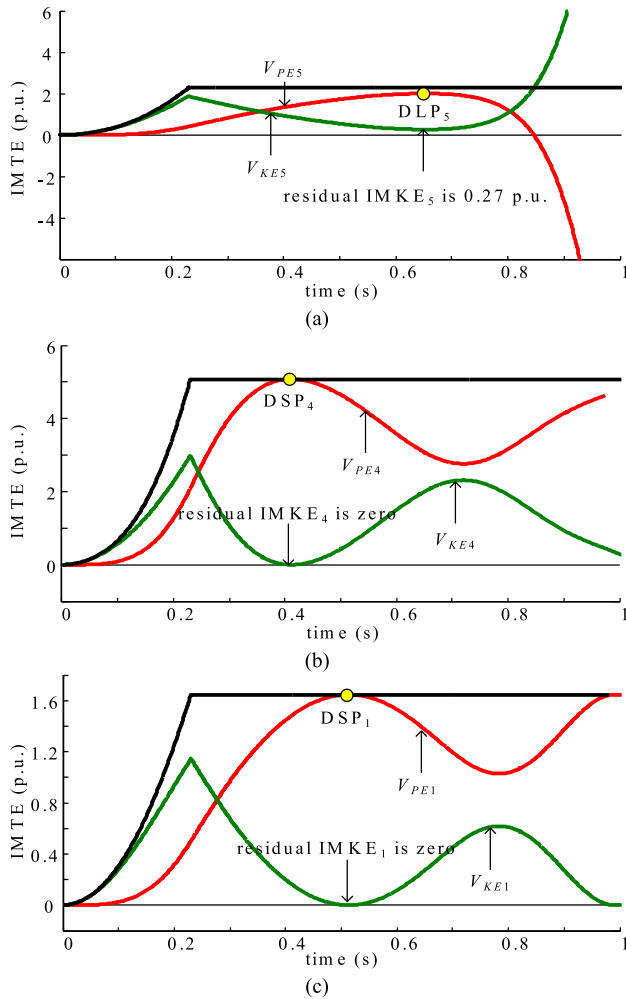

(a)

(b)

(c)

FIGURE 23. Transient energy conversion inside each critical machine [TS-1, bus-19, 0.230 s]. (a) Machine 5. (b) Machine 4. (c) Machine 1.

In particular, Machine 5 becomes unstable because residual IMKE_5 occurs at DLP_5 (0.27 p.u.), while Machines 4 and 1 remain stable because the residual IMKE_4 and residual IMKE_1 are strictly zero at their DSPs. The stability of each machine is characterized precisely at its MPP, as shown in Fig. 23. The trajectory of the machine is also depicted clearly at its MPP, as in Fig. 22. In the end, the entire

FIGURE 24. Transient energy conversion inside Machine 4 when the energy reference point is changed.

multimachine system is evaluated to go unstable because Machine 5 becomes unstable at DLP_5, according to the unity principle (MAP-VIII).

C. DEMONSTRATION ABOUT MAP-IV

The independent parallel stability characterization in the individual-machine transient stability analysis is of interest because it indicates that the energy reference point of each machine does *not* need to be set as the same.

Using the case in Section B as an example, assume the energy reference point of Machine 4 is set as θ^c rather than θ^s. The modified IMTE_4 is shown in Fig. 24.

From Fig. 24, compared with the case in Section B, the characteristics of the modified IMTE_4 are given as follows:

(i) The IMKE_4 curve remains unchanged.

(ii) IMPE_4 reaches zero at the fault clearing point rather than the SEP.

(iii) The IMPE_4 curve and IMTE_4 curve move downward by the same distance ($\int_{\theta_4^s}^{\theta_4^c} \left[-f_4^{(PF)} \right] d\theta_4 = 2.088$ p.u.).

Following (i) to (iii), the residual IMKE_4 remains strictly zero at DSP_4 after the change of the energy reference point, and thus Machine 4 is still precisely characterized as maintaining stable. This fully indicates that the "energy conversion" inside Machine 4 remains the same as that in Fig. 23 (b), although the value of the "energy" is changed.

VI. FURTHER DISCUSSIONS
A. CLARIFICATION OF THE POTENTIAL ENERGY SURFACE

In the original Newtonian system, as shown in Fig. 2, the basin is physically "real", and it is simply used to depict the position of the ball (h_i). In the individual machine transient stability analysis, the IMPES is also seen as a "basin" with a ball rolling on it [19]. However, the authors state that the two concepts are completely different. The clarification is given below.

We focus on the modeling of the IMPES [19]. Assume numerous system trajectories in the angle space form a "system-trajectory set". Then, the IMPE of an individual machine is computed along each system trajectory in the set.
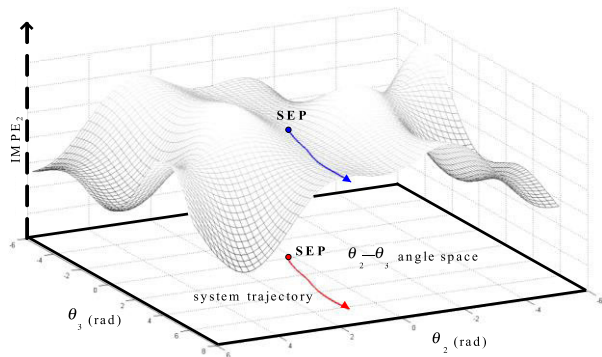
FIGURE 25. Formations of IMPES$_2$ in TS-4.

FIGURE 26. Occurrence of UEP in the generalized Newtonian system.

FIGURE 27. Net force of each machine along the time horizon.

In this way, the IMPE of the machine under different system trajectories will form the IMPES.

The IMPES of a machine is shown in Fig. 25

From Fig. 25, the IMPES is modeled in a genuine IMPE manner. The "altitude" of the IMPES represents the IMPE (V_{PE2}) rather than the position (θ_2) of the machine. In addition, the IMPES is separated by flat land along the constant-θ_i angle surface [19]. Therefore, the IMPES should be seen as a distinctive "energy basin" with "gaps". This is completely different from the physically real basin in the Newtonian system that simply depicts the position of a ball (h_i).

B. THE SECOND DEFECT OF UEP

In Ref. [19], an inherit defect of the unstable equilibrium point (UEP) is exposed through the concept of the zero-f_i angle surface. That is, some UEPs physically do *not* exist in a multimachine power system. In this section, from the perspective of the Newtonian system, another defect of UEP is exposed. That is, the UEP completely ignores the unique and different NEC characteristics inside each machine.

This defect can be explained by using the generalized Newtonian system. The UEP and SEP are mathematically given as

$$f_i(\boldsymbol{h}) = 0 \quad i = 1, 2 \ldots n \quad (39)$$

Following the definition of the DLP with zero gravity as given in Section II F, the occurrence of UEP can be depicted as follows:

(i) Each unstable machine in the system reaches its corresponding DLP.

(ii) Each stable machine in the system reaches its corresponding zero-f_i point.

In fact, (i) and (ii) will form an extreme scenario. In this scenario, each machine reaches the zero-gravity point (DLP or zero-f_i point) "simultaneously". In particular, each unstable machine lies in its IMPEB, and it is ready to become unstable, while each stable machine oscillates with zero-f_i.

A demonstration of this extreme scenario in the Newtonian system is shown in Fig. 26.

From Fig. 26, at the moment that UEP occurs (t_{UEP}), Machines 1 and 3 lie in their DLPs, while Machine 2 lies in
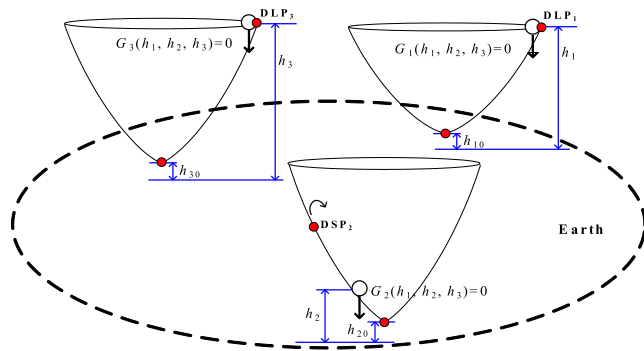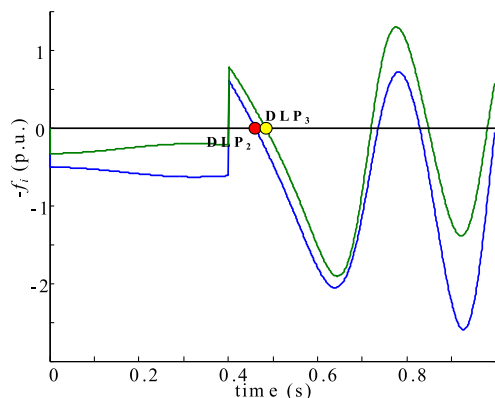
the zero-f_2 point. Then, at $t_{\text{UEP}} + \Delta t$, this fragile balance is completely destroyed because of the motion of each machine. Against this background, Machines 1 and 3 fall into their reverse gravity fields "simultaneously", and they become unstable. Meanwhile, Machine 1 still oscillates around the bottom of the basin.

Frankly, this extreme scenario will never occur along the actual simulated postfault system trajectory, because it completely ignores the unique and different NEC characteristics inside each machine. The case [TS-4, bus-1, 0.40 s] in Section III C is used as an example. The variance in f_i of each machine along the time horizon is shown in Fig. 27. Note that this figure is not the Kimbark curve of the machine. The variance in $f_i^{(PF)}$, i.e., the "gravity" of each machine along the time horizon, is shown in Fig. 28. The system trajectory is already shown in Fig. 13. Detailed transient stability analysis was already given in Ref. [19].

From Fig. 27, because of the complicated interactions among all machines in the system, the NEC inside each machine is unique and different, and thus, the occurrence of the DLP of each unstable critical machine is also different. Against this background, all DLPs cannot occur simultaneously. Instead, they will occur one after another along the time horizon. In particular, in this simulation case, DLP$_2$ and DLP$_3$ occur at 0.47 s and 0.49 s, respectively.

From the analysis above, UEP is a "fictional" and "static" concept that is computed only through mathematics ($\boldsymbol{f}(\boldsymbol{h}) = \boldsymbol{0}$). The UEP completely ignores the distinctive
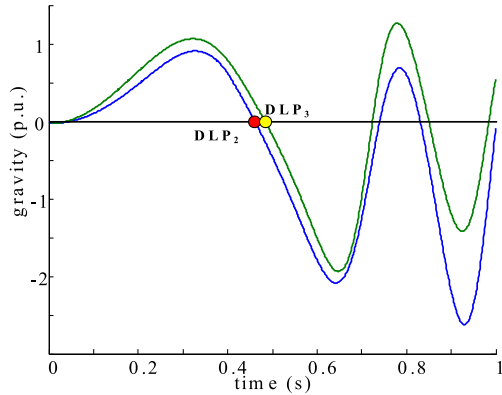
FIGURE 28. Gravity of each machine along the time horizon.

NEC characteristics inside each machine and does *not* exist along the actual postfault system trajectory. Therefore, UEP cannot be used as the critical energy point of a generalized Newtonian system.

C. DISCUSSION OF THE MOTION REFERENCE

1) EARTH REFERENCE

In the Newtonian system, the Earth is set as the motion reference to depict the relative motion of each ball in the system. Against this background, the NEC of each ball measures the "relative motion" between the ball and the Earth.

2) COI-SYS REFERENCE

Following the mappings between the Newtonian system and the multimachine power system as analyzed in Section IV, the COI-SYS is naturally used as the motion reference, i.e., "Earth", to measure the relative motion of each machine. Against this background, the transient energy conversion of each machine measures "relative motion" between each real machine and COI-SYS.

3) REAL MACHINE REFERENCE

We go a step further. Based on the original idea of the "relative motion", it is certain that a physically real machine can also be used as the motion reference of the entire system, even though it is neither infinitely large (such as the Earth) nor equivalent (such as COI-SYS). This real machine is named the "reference machine" (RM) [17]. Against this background, the transient energy conversion inside each machine measures the "relative motion" between the real machine and RM. Note that the RM will become "relatively stationary" once it is set as the motion reference of the entire system, even though it has velocity in the synchronous reference.

Tutorial comparisons between the COI-SYS reference and RM reference are shown in Figs. 29 and 30, respectively. The simulation case is [TS-1, bus-21, 0.370 s] [17]. The formation of the generalized Newtonian system using the RM as the motion reference is shown in Fig. 31.
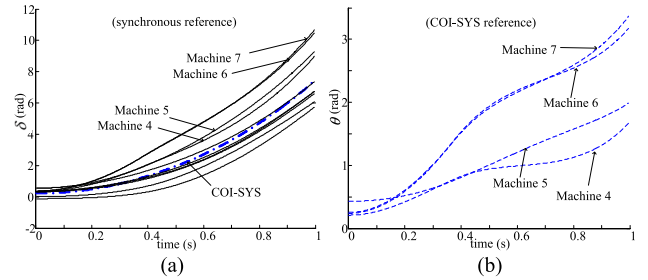

FIGURE 29. Trajectory separation using the COI-SYS reference. (a) System trajectory in the synchronous reference. (b) IMTR of each critical machine using the COI-SYS reference.
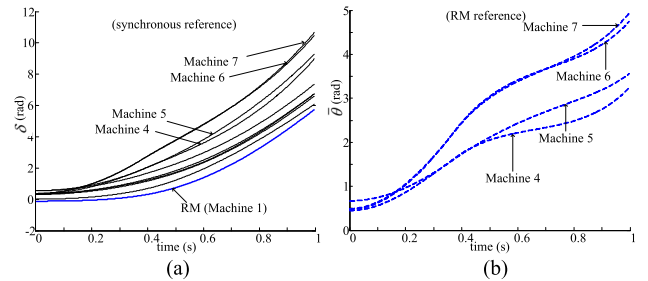

FIGURE 30. Trajectory separation using the RM reference. (a) System trajectory in the synchronous reference. (b) IMTR of each critical machine using the RM reference.
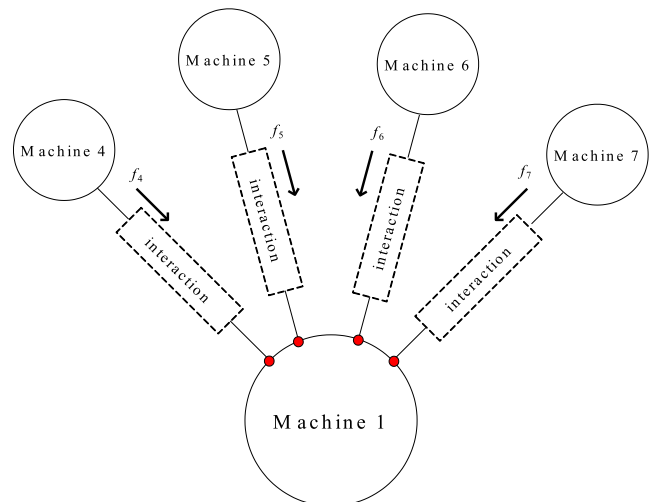

FIGURE 31. Formation of the Newtonian system using the RM as the Earth.

From Figs. 29 and 30, quite different from the COI-SYS reference, the physically real Machine 1 is set as the RM and is used as the motion reference of the entire system [17]. Against this background, the individual-machine transient stability analysis is completely transferred from the COI-SYS reference to the RM reference. The stability of each critical machine is also characterized independently in parallel in the RM reference.

From the analysis above, theoretically, the mechanisms of the individual-machine transient stability under the two references are quite similar. However, technically, the distinctive advantage of the RM is that the concept of the equivalent COI-SYS is completely eliminated from the individual-machine
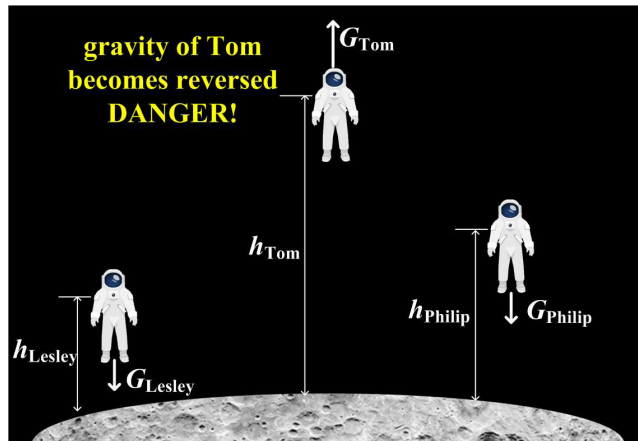
FIGURE 32. Variant gravity in the Stanton planet.

transient stability analysis. In particular, the stability of each machine in the RM reference is measured through only two "real" machines without using the equivalent COI-SYS that comprises the information of all machines in the system, which greatly improves the efficiency of TSA. This also indicates that the motion reference in the original Newtonian system can be set as a physically real ball rather than the infinitely large Earth.

D. STANTON PLANET

In our daily living environment, the "value" and the "direction" of the gravitational field are constant because the Earth is a "gravity-constant" planet. In this section, a virtual planet is established by the authors. This planet is named the "Stanton" planet to commemorate the contributions of Dr. Stanton in individual machine studies [4], [5], [12], [13].

The Stanton planet strictly follows the modeling of the generalized Newtonian system. It is formed by the planet itself and all the objects on it. Compared with gravity-constant Earth, the Stanton planet is a "gravity-variant" planet. That is, the gravity of each object is affected by the altitudes of all the objects (including the object itself) on this planet. In particular, the direction of gravity might reverse if the object leaves far from the ground.

Assume three astronauts, i.e., Lesley, Tom and Philip, land on the Stanton planet. The three astronauts and the Stanton planet naturally form a generalized Newtonian system with four components. Then, two actions of the astronauts are given as follows:

Walk: Under this circumstance, the altitude of each astronaut is zero ($h_i = 0$), and thus, the gravity of each astronaut is also zero ($G_i(\boldsymbol{h}) = 0$). The three astronauts remain on the ground and they are safe.

Jump: Bored with walking, the three astronauts try a very dangerous action. That is, they jump up from the ground. Tom jumps much harder and higher than the other two astronauts.

At first, the gravity imposed on Tom remains positive because the altitude is low. He is decelerating, and the gravitational field feels "similar" to the Earth. However,

the situation becomes dangerous after a while. With increasing altitude, Tom goes through his "DLP", and his gravity reverses. After that, he keeps accelerating and finally separates from the planet. Comparatively, the gravities imposed on Lesley and Philip remain downward. The two finally fall back to the ground.

In the end, Lesley and Philip found that they might live flexibly on this planet. However, they should always remember "no jumping" when hiking on this distinctive gravity-variant planet.

A demonstration of the variant gravity of the Stanton planet is shown in Fig. 32.

VII. CONCLUSION

In this paper, the authors clarify that Newtonian mechanics can be used as the theoretical foundation of individual-machine transient stability. The NEC strictly holds inside the original Newtonian system. It is clarified that EAC is the Newtonian work, and the EAC is identical to the NEC. Based on these features, the stability characterizations of the original Newtonian system are given. It is shown that NEC is independent of the setting of the energy reference point. Furthermore, a generalized Newtonian system with multiple balls is established. The generalized Newtonian system can be decomposed into multiple two-ball-based subsystems. In this way, independent parallel stability characterization is used in each subsystem after decomposition. Finally, eight strict mappings between Newtonian system stability and individual-machine transient stability are analyzed. In addition, the difference between the physically real basin in the Newtonian system and the IMPES is clarified. The second defect of UEP is also exposed through the modeling of the generalized Newtonian system. The gravity-variant Stanton planet visually explains the mechanisms of the generalized Newtonian system. All the analyses in this paper validate that the theoretical foundation of the individual-machine transient stability should be Newtonian mechanics.

In the history of power system transient stability, global methods and individual-machine methods seem to be developed "independently". However, the thinking of Newtonian mechanics in both global methods and individual-machine methods strongly indicates that "transient stability paradigms" can be found between them. The exploration of these paradigms will bring real unity between global thinking and individual-machine thinking. This will be analyzed in future work.

REFERENCES

[1] T. Athay, R. Podmore, and S. Virmani, "A practical method for the direct analysis of transient stability," *IEEE Trans. Power App. Syst.*, vol. PAS-98, no. 2, pp. 573–584, Mar. 1979.

[2] N. Kakimoto, Y. Ohsawa, and M. Hayashi, "Transient stability analysis of electric power system via Lur's type Lyapunov function, Part I new critical value for transient stability," *IEE Trans. Jpn.*, vol. 98, nos. 5–6, pp. 63–71, 1978.

[3] N. Kakimoto, Y. Ohsawa, and M. Hayashi, "Transient stability analysis of electric power system via Lur's type Lyapunov function, Part II modification of Lure type Liapunov function with effect of transfer conductances," *IEE Trans. Jpn.*, vol. 98, nos. 5–6, pp. 72–79, 1978.

[4] A. A. Fouad and S. E. Stanton, "Transient stability of a multi-machine power system Part I: Investigation of system trajectories," *IEEE Trans. Power App. Syst.*, vol. PAS-100, no. 7, pp. 3408–3416, Jul. 1981.

[5] A. Fouad and S. Stanton, "Transient stability of a multi-machine power system. Part II: Critical transient energy," *IEEE Trans. Power App. Syst.*, vols. PAS-100, no. 7, pp. 3417–3424, Jul. 1981.

[6] Y. Xue, "Re-examination of transient energy functions and critical energy," *Automat. Electr. Power Syst.*, vol. 6, pp. 9–18, Jun. 1991.

[7] D.-Z. Fang, T. S. Chung, Y. Zhang, and W. Song, "Transient stability limit conditions analysis using a corrected transient energy function approach," *IEEE Trans. Power Syst.*, vol. 15, no. 2, pp. 804–810, May 2000.

[8] M. Yin, C. Y. Chung, K. P. Wong, Y. Xue, and Y. Zou, "An improved iterative method for assessment of multi-swing transient stability limit," *IEEE Trans. Power Syst.*, vol. 26, no. 4, pp. 2023–2030, Nov. 2011.

[9] M.Ribbens-Pavella, D. Ernst, and D. Ruiz-Vega, *Transient Stability of Power Systems: A Unified Approach to Assessment and Control*. Norwell, MA, USA: Kluwer, 2000.

[10] V. Vittal, "Power system transient stability using critical energy of individual machines," Ph.D. dissertation, Dept. Elect. Eng., Iowa State Univ., Ames, IA, USA, 1982.

[11] A. Michel, A. Fouad, and V. Vittal, "Power system transient stability using individual machine energy functions," *IEEE Trans. Circuits Syst.*, vol. 30, no. 5, pp. 266–276, May 1983.

[12] S. E. Stanton and W. P. Dykas, "Analysis of a local transient control action by partial energy functions," *IEEE Trans. Power Syst.*, vol. 4, no. 3, pp. 996–1002, Aug. 1989.

[13] S. E. Stanton, "Transient stability monitoring for electric power systems using a partial energy function," *IEEE Trans. Power Syst.*, vol. 4, no. 4, pp. 1389–1396, Nov. 1989.

[14] R. Ando and S. Iwamoto, "Highly reliable transient stability solution method using energy function," *IEE Trans. Jpn.*, vol. 108, no. 4, pp. 253–260, Jun. 1988.

[15] S. Wang, J. Yu, and W. Zhang, "Transient stability assessment using individual machine equal area criterion PART I: Unity principle," *IEEE Access*, vol. 6, pp. 77065–77076, 2018.

[16] S. Wang, J. Yu, and W. Zhang, "Transient stability assessment using individual machine equal area criterion PART II: Stability margin," *IEEE Access*, vol. 6, pp. 38693–38705, 2018.

[17] S. Wang, J. Yu, and W. Zhang, "Transient stability assessment using individual machine equal area criterion PART III: Reference machine," *IEEE Access*, vol. 7, pp. 80174–80193, 2019.

[18] S. Wang, J. Yu, A. M. Foley, and W. Zhang, "Transient energy of an individual machine PART I: Stability characterization," *IEEE Access*, vol. 9, pp. 44797–44812, 2021.

[19] S. Wang, J. Yu, A. M. Foley, and W. Zhang, "Transient energy of an individual machine PART II: Potential energy surface," *IEEE Access*, vol. 9, pp. 60223–60243, 2021.

[20] Z. Liu and Z. Zhang, "Quantifying transient stability of generators by basin stability and Kuramoto-like models," in *Proc. North Amer. Power Symp. (NAPS)*, Sep. 2017, pp. 1–6.

[21] K. Sun, S. T. Lee, and P. Zhang, "An adaptive power system equivalent for real-time estimation of stability margin using phase-plane trajectories," *IEEE Trans. Power Syst.*, vol. 26, no. 2, pp. 915–923, May 2011.

SONGYAN WANG received the B.S., M.S., and Ph.D. degrees from the School of Electrical Engineering and Automation, Harbin Institute of Technology (HIT), in 2007, 2009, and 2012, respectively. He was a Visiting Scholar with Virginia Tech, Blacksburg, VA, USA, in 2010. From 2013 to 2014, he was a Research Fellow with Queen's University Belfast, U.K. He is currently an Assistant Professor with HIT. His research interests include power system operation and control. He is also an Associate Editor of *Renewable and Sustainable Energy Reviews*.

JILAI YU joined the School of Electrical Engineering and Automation, Harbin Institute of Technology, in 1992. From 1994 to 1998, he was an Associate Professor with the School of Electrical Engineering and Automation, where he is currently a Professor and the Director of the Electric Power Research Institute. His research interests include power system analysis and control, optimal dispatch of power systems, green power, and smart grids.

AOIFE M. FOLEY (Senior Member, IEEE) received the B.E. degree in civil engineering from the Irish Power System, University College Cork, Ireland, in 1996, the M.Sc. degree in transportation engineering from the Trinity College Dublin, The University of Dublin, Ireland, in 1999, and the Ph.D. degree in unit commitment modeling of wind and energy storage from the Irish Power System, University College Cork, in 2011. She worked in industry for a period of 12 years with ESB International, Siemens, SWS Energy, and PM Group, mostly in the planning, design, and project management of energy, telecoms, waste, and pharma projects. She is currently a Reader with the School of Mechanical and Aerospace Engineering, Queen's University Belfast, U.K. Her research interests include energy system modeling focused on electricity systems, markets and services, wind power, electric vehicles, and smart technologies. She was a Founding Member of the IEEE VTS, U.K., and the Ireland Chapter, in 2011. She is also a Chartered Engineer, in 2001, a fellow of the Engineers Ireland, in 2012, and a member of the IEEE PES and the IEEE VTS. She is also the Editor-in-Chief of *Renewable and Sustainable Energy Reviews*.

• • •